PAPER Special Section on Wideband Systems

Performance Analysis of MIMO/FSO Systems Using SC-QAM Signaling Over Atmospheric Turbulence Channels**

Ha D. TRUNG†, *Nonmember and* **Anh T. PHAM**††*, *Member*

SUMMARY We theoretically analyze the performance of multiple-input multiple-output (MIMO) free-space optical (FSO) systems using subcarrier quadrature modulation (SC-QAM) signaling. The system average symbol-error rate (ASER) is derived taking into account the atmospheric turbulence effects on the MIMO/FSO channel, which is modeled by log-normal and the gamma-gamma distributions for the cases of weak-to-strong turbulence conditions. We quantitatively discuss the influence of turbulence strength, link distance, and different MIMO configurations on the system ASER. We also analytically derive and discuss the MIMO/FSO average (ergodic) channel capacity (ACC), which is expressed in terms of average spectral efficiency (ASE), under the impact of various channel conditions.

key words: *Free-space optical (FSO) communications, multiple-input multiple-output (MIMO), subcarrier quadrature-amplitude modulation (SC-QAM), atmospheric turbulence, channel capacity.*

1. Introduction

Free-space optical (FSO) communications, also known as optical-wireless communication, is a cost-effective, license-free, high security and high bandwidth access technique, which has received considerable attention recently for a variety of applications [1]–[3]. In spite of the major advantages of FSO communications, its widespread use is hampered by several challenges in practical deployment. For example, aerosol scattering caused by rain, fog, and snow results in degrading the system performance, leaving the FSO link vulnerable to unfavorable weather conditions [4].

One of major impairments to the performance of FSO systems is the influence of atmospheric turbulence [5], which will be the focus of this paper. Atmospheric turbulence caused by variations in the refractive index due to inhomogeneties in temperature, pressure fluctuations, humidity changes, and motion of the air along the propagation path of the laser beam. This results in irradiance fluctuations in the received signal, i.e., the signal fading, which severely degrades the system performance. Therefore, powerful fading-mitigation techniques need to be deployed for FSO links particularly with transmission distances of 1 km or longer [6]. Error-control coding in conjunction with interleaving can be employed in FSO communications to combat fading phenomenon [7], [8].

Manuscript received March 15, 2013.

†The author is with School of Electronics and Telecommunications, Hanoi University of Science and Technology, Vietnam.

††The author is with the Computer Communications Lab., University of Aizu, Aizuwakamatsu-shi, Fukushima 965-8580, Japan.

*E-mail: pham@u-aizu.ac.jp

**The paper is presented in part at IEEE ICC 2013.

DOI: 10.1587/trans.E0.??.1

Recent works have shown that, similar to radio communications, the effect of fading over FSO links can be significantly reduced by employing a multiple-input multiple-output (MIMO) FSO system with multiple lasers at the transmitter and multiple photodetectors at the receiver. The first use of space diversity on FSO systems has been proposed in [9]. In [10], [11] Lee, Shin and Chan have derived the outage probability of MIMO/FSO systems over log-normal turbulence channels assuming Gaussian noise statistics that can be considered as a limiting case of Poisson statistics. In [12], [13] Wilson *et al*. have formulated and analyzed symbol-error probability (SEP) and bit-error probability (BEP) of MIMO/FSO transmissions assuming pulse-position modulation (PPM) and Q-ary PPM in both log-normal and Rayleigh fading channels. In [14] Navidpour *et al*. have investigated the bit-error rate (BER) performance of MIMO/FSO links for both independent and correlated log-normal atmospheric turbulence channels. In [15], under the assumption of intensity-modulation/direct-detection (IM/DD) with on-off keying (OOK), a closed-form expression for the BER expression of single-input single-output (SISO) case and approximated closed-form BER expressions of MIMO/FSO links over strong turbulence channels in terms of Meijer's G-functions have been investigated. However, most of existing works have mainly employed OOK and PPM modulation techniques due to its simplicity and low cost. Whereas, because of the presence of atmospheric turbulence, OOK modulation requires to select adaptive thresholds appropriately to achieve its optimal performance and PPM modulation has a poor bandwidth efficiency.

To overcome the limitations of OOK and PPM, subcarrier intensity modulation schemes, such as subcarrier phase-shift keying (SC-PSK) and quadrature-amplitude modulation (SC-QAM), have been proposed to modulate several digital streams from the same source onto different radio-frequency (RF) subcarrier frequencies. The combined signal is then applied to vary the laser irradiance in order to achieve higher system capacity by employing each RF subcarrier frequency to a different data source. PSK has been first proposed as an alternative modulation technique for FSO communication systems by Huang *et al*. in [16]. Thereafter, the performance of PSK intensity modulated FSO communications has been extensively investigated [17]-[22]. Besides the PSK modulation, QAM has also gained attention over FSO links. High spectral efficiency is the main advantage of QAM since a 2^K-QAM constellation has K times

the spectral efficiency of a binary PSK constellation. In [23], [24] Cvijetic and Bekkali studied mathematical average SEP and BEP of orthogonal frequency-division multiplexing (OFDM) signals over nonfading and fading FSO link for different types of modulation, including QPSK, 16-QAM, and 64-QAM. In [25] Hassan *et al*. presented the ASER for subcarrier intensity modulated wireless optical communications with general order rectangular QAM by using the series expansion of the modified Bessel function [26]. Furthermore, average SEP of general-order rectangular QAM of FSO system over atmospheric turbulence channels can be found in [27], [28]. Most recently, the SEP and BER analyses of FSO systems with avalanche photodiode (APD) receiver over atmospheric turbulence channel have been reported [29], [30]. However, to the best of our knowledge, the performance analysis of MIMO/FSO systems using SC-QAM signaling has not been appeared in the literature.

In this paper, our goal is to study the performance of MIMO/FSO systems employing SC-QAM signaling over atmospheric turbulence channels. The average symbol-error rate (ASER) are theoretically derived when both log-normal and the gamma-gamma distributions are used to model the cases of weak-to-strong turbulence conditions. Based on our analytical solution of derived formulas, it is feasible to evaluate the ASER for specific parameters of the free-space optical links. Various numerical results are presented that demonstrate our mathematical analysis. Moreover, we also analytically derive and discuss the MIMO/FSO average (ergodic) channel capacity (ACC), which is expressed in terms of average spectral efficiency (ASE), under the impact of various channel conditions and system parameters.

The remainder of the paper is organized as follows. In Section 2, the system descriptions and channel models are presented. In Section 3, the performance analysis on the ASER of MIMO/FSO systems using SC-QAM signaling is evaluated for weak-to-moderate and moderate-to-strong turbulence channels modeled by the log-normal and the gamma-gamma distributions, respectively. The system ACC is also presented in this Section. The numerical results are provided in Section 4. Finally, the paper concludes with a summary given in Section 5.

2. System Descriptions

2.1 FSO System using SC-QAM

The FSO system using SC-QAM signaling with single transmitter and single receiver (SISO system) is described in Fig. 1a. In this system, QAM symbol is first used to modulate a subcarrier frequency f_c; this electrical subcarrier QAM signal is then used to modulate the intensity of a laser. Generally, the electrical QAM signal can be given by

$$e(t) = s_I(t)\cos(2\pi f_c t) - s_Q(t)\sin(2\pi f_c t),\ 0 \le t \le T_s \qquad (1)$$

where $s_I(t) = \sum_{i=-\infty}^{\infty} a_i(t)g(t-iT_s)$ is the in-phase signal and $s_Q(t) = \sum_{j=-\infty}^{\infty} b_j(t)g(t-jT_s)$ is the quadrature signal; $a_i(t)$ and

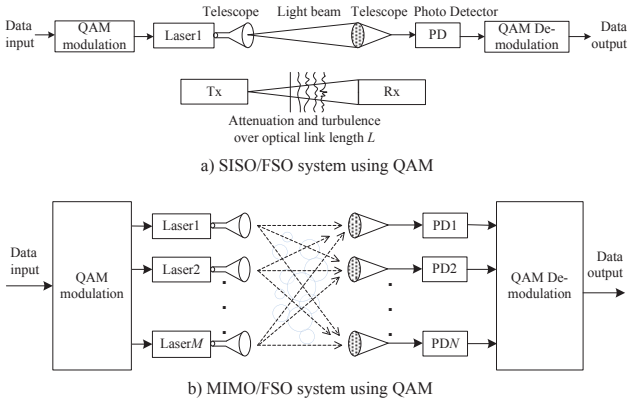

Fig. 1 Block diagram of $M\times N$ MIMO/FSO communication system using SC-QAM signaling over atmospheric turbulence channel

$b_j(t)$ are the in-phase and the quadrature information signal amplitudes of the transmitted data symbol, respectively; $g(t)$ is the signal shaping pulse, and T_s is the symbol interval. Equivalently, the transmitted optical intensity can be given as

$$s(t) = P_s\{1+\kappa[s_I(t)\cos(2\pi f_c t) - s_Q(t)\sin(2\pi f_c t)]\}, \qquad (2)$$

where κ is the modulation index and $0 < \kappa \le 1$. P_s denotes the average optical power per symbol. The received optical intensity, after being distorted over the turbulence channel, can be written as

$$r(t) = XaP_s\{1+\kappa[s_I(t)\cos(2\pi f_c t) - s_Q(t)\sin(2\pi f_c t)]\}. \qquad (3)$$

In this equation, a is the atmospheric attenuation factor, X represents the signal scintillation caused by atmospheric turbulence and can be modeled as a stationary random process. The DC term $\{aP_sX\}$ can be filtered out by a bandpass filter. The electrical signal at the photodetector (PD) output can be expressed as

$$r_e(t) = Xa\Re P_s\kappa e(t) + \upsilon(t), \qquad (4)$$

where $\Re$ denotes the PD's responsivity; $\upsilon(t)$ is receiver noise, which can be modeled as additive white Gaussian noise (AWGN) process with power spectral density N_0. Electrical signal is then QAM demodulated and sampled to recover the original data.

2.2 MIMO/FSO System using SC-QAM

In this section, we consider a general $M\times N$ MIMO/FSO system using SC-QAM signaling with M lasers pointing toward an N-aperture receiver as depicted in Fig. 1b. Data transmission with the same SC-QAM signal is transmitted with perfect synchronization by each of the M telescopes through an turbulence channel toward N PDs. The light beam-width of each telescope is assumed to be wide enough to illuminate the entire receiver array. The transmitter's telescope array is assumed to produce the same total optical power irrespective of M to enforce a fair comparison with

the single transmitter case. The distance between the each transmitting telescope to the receiving one is assumed to be sufficient so that spatial correlation is negligible.

The MIMO/FSO channel can be modeled by an $M \times N$ matrix of the turbulence channel, denoted as $\mathbf{X} = [X_{mn}]_{m,n=1}^{M,N}$. Similar to Eq. 4, the electrical signal at the input of the QAM demodulator can be expressed as follows

$$r_e(t) = a\Re P_s \kappa e(t) \sum_{m=1}^{M} \sum_{n=1}^{N} X_{mn} + \upsilon(t), \;\; n = 1, 2..., N, \quad (5)$$

where $e(t)$ represents the QAM signal and $\upsilon(t)$ is the total receiver noise as defined above. X_{mn} denotes the stationary random process for the turbulence channel from the mth laser to the nth PD. When the equal gain combining (EGC) detector is employed at the receiver to estimate the transmitted signal, the instantaneous electrical SNR can be expressed as a finite sum of sub-channels as

$$\gamma = \left(\sum_{m=1}^{M} \sum_{n=1}^{N} \sqrt{\gamma_{mn}} \right)^2, \quad (6)$$

where γ_{mn} is the random variable (r.v.) defined as the instantaneous electrical SNR component of the sub-channel from the mth laser to the nth PD, and it can be expressed as

$$\gamma_{mn} = \frac{(\frac{1}{MN} X_{mn} a\Re P_s \kappa)^2}{N_0} = \overline{\gamma}_{mn} X_{mn}^2, \quad (7)$$

in which, we denote $\overline{\gamma}_{mn}$ as the average electrical SNR contributed by the sub-channel between the mth laser and the nth PD. $\overline{\gamma}_{mn}$ is given by $\overline{\gamma}_{mn} = (\frac{1}{MN} a\Re P_s \kappa)^2 / N_0$.

2.3 Atmospheric Turbulence Channel Models

When optical signal propagates through the FSO channel, the signal's amplitude and phase are fluctuated due to the atmospheric turbulence. For weak atmospheric turbulence conditions, the turbulence induced scintillation is assumed to be a random process that follows the log-normal distribution [27]; whereas for moderate-to-strong turbulence conditions, a gamma-gamma distribution is used [31].

2.3.1 Log-normal Turbulence Model

In the log-normal turbulence channel, assuming that the average of scintillation is normalized to unity, the probability density function (p.d.f) for r.v. X_{mn} representing the turbulence of the sub-channel between the mth laser and the nth receiver can be described as [27]

$$f_{X_{mn}}(x) = \frac{1}{x\sigma_s \sqrt{2\pi}} \exp\left(-\frac{(\ln(x) + \frac{\sigma_s^2}{2})^2}{2\sigma_s^2} \right), \quad (8)$$

where $\sigma_s^2 = \exp(\psi_1 + \psi_2) - 1$ with ψ_1 and ψ_1 being respectively given by

$$\psi_1 = \frac{0.49\sigma_2^2}{(1 + 0.18d^2 + 0.56\sigma_2^{12/5})^{7/6}}, \quad (9)$$

and

$$\psi_2 = \frac{0.51\sigma_2^2 (1 + 0.69\sigma_2^{12/5})^{-5/6}}{1 + 0.9d^2 + 0.62d^2\sigma_2^{12/5}}. \quad (10)$$

In Eqs. (9) and (10), $d = \sqrt{kD^2/4L}$, where $k = 2\pi/\lambda$ is the optical wave number, L is the link distance in meters, λ is the optical wavelength, and D is the receiver aperture diameter of the PD. The parameter σ_2^2 is the Rytov variance and in this case, is expressed by [31]

$$\sigma_2^2 = 0.492 C_n^2 k^{7/6} L^{11/6}, \quad (11)$$

where C_n^2 stands for the strength of the atmospheric turbulence, which is altitude-dependent and varies from 10^{-17} to $10^{-13} \mathrm{m}^{-2/3}$ accordingly to the turbulence conditions.

2.3.2 Gamma-Gamma Turbulence Model

For the case of the gamma-gamma channel, the p.d.f of a normalized gamma-gamma r.v. X_{mn} is given as [31]

$$f_{X_{mn}}(x) = \frac{2(\alpha\beta)^{\frac{\alpha+\beta}{2}}}{\Gamma(\alpha)\Gamma(\beta)} x^{\frac{\alpha+\beta}{2}-1} K_{\alpha-\beta}\left(2\sqrt{\alpha\beta x}\right), \quad (12)$$

where $\Gamma(\cdot)$ is the Gamma function and $K_{\alpha-\beta}(\cdot)$ is the modified Bessel function of the second kind of order $(\alpha - \beta)$, while the parameters α and β are directly related to atmospheric conditions through the following expression:

$$\alpha = \left[\exp(\psi_1) - 1\right]^{-1}, \beta \quad = \left[\exp(\psi_2) - 1\right]^{-1}. \quad (13)$$

The parameters α and β are related with the scintillation index by

$$SI = \frac{1}{\alpha} + \frac{1}{\beta} + \frac{1}{\alpha\beta}. \quad (14)$$

Fig. 2 shows the p.d.f for a few instances of the turbulence strength. For $SI < 0.8$, the gamma-gamma distribution resembles a log-normal distribution. The gamma-gamma distributions with turbulence strength values of $SI = 0.8$, $SI = 1.2$, and $SI = 2.0$ are quite different with smaller amplitudes than the log-normal distributions in two specific cases of $SI = 0.45$ and $SI = 0.55$. In particular, the gamma-gamma model has higher density in the low amplitude region, resulting in a more unexpected impact on the system performance.

3. Performance Analysis

3.1 ASER Derivation

The atmospheric turbulence channel can be modeled as a slow-fading process because its temporal correlation time,

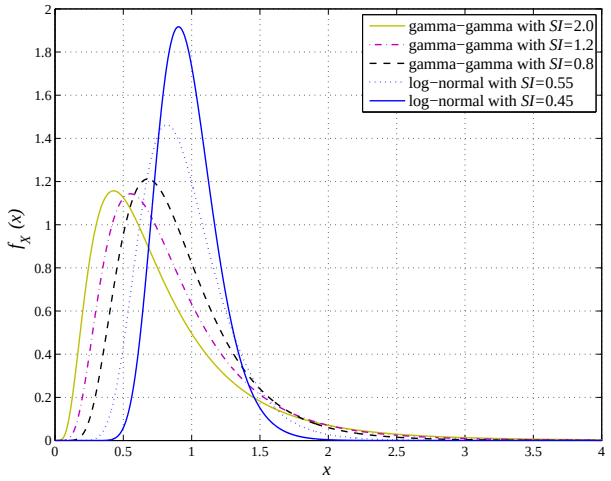

Fig. 2 p.d.fs of several log-normal and gamma-gamma intensity distributions

which is on the order of several milliseconds, is much larger than the QAM symbol duration. The ASER averaged over the turbulence channel therefore can be expressed as

$$\overline{P}_{se}^{MIMO} = \int_{\mathbf{\Gamma}} P_e(\gamma) \times f_{\mathbf{\Gamma}}(\Gamma) d\Gamma. \tag{15}$$

Here, γ is the instantaneous electrical SNR, which is a function of γ_{mn} as given in Eq. (6). $\mathbf{\Gamma} = \{\Gamma_{nm}, n = 1, ..., N, m = 1, ..., M\}$ is the matrix of the MIMO atmospheric turbulence channels. $P_e(\gamma)$ is the conditional error probability (CEP) of the received instantaneous electrical SNR. For SC-QAM systems, the CEP $P_e(\gamma)$ is given by [32]

$$P_e(\gamma) = 1 - \Big[1 - 2q(M_I)Q(A_I\sqrt{\gamma})\Big]\Big[1 - 2q(M_Q)Q(A_Q\sqrt{\gamma})\Big], \tag{16}$$

where M_I and M_Q are respectively in-phase and quadrature signal amplitudes, $q(x) \triangleq 1 - x^{-1}$, $Q(x) \triangleq 1/\sqrt{2\pi}\int_x^{\infty} \exp(-t^2/2)dt$ is the Gaussian Q-function which relates to the terms of the complementary error function erfc$(\cdot)$ by $Q(x) = \frac{1}{2}\text{erfc}(x/\sqrt{2})$, $A_I = (6/[(M_I^2 - 1) + r^2(M_Q^2 - 1)])^{1/2}$, and $A_Q = (6r^2/[(M_I^2 - 1) + r^2(M_Q^2 - 1)])^{1/2}$, in which $r = d_Q/d_I$ is the quadrature to in-phase decision distance ratio.

Equation (16) can further be written as follows

$$\begin{aligned} P_e(\gamma) = {} & 2q(M_I)Q(A_I\sqrt{\gamma}) + 2q(M_Q)Q(A_Q\sqrt{\gamma}) \\ & - 4q(M_I)q(M_Q)Q(A_I\sqrt{\gamma})\,Q(A_Q\sqrt{\gamma}). \end{aligned} \tag{17}$$

Replace (17) into (15), ASER of the MIMO systems can be derived as

$$\begin{aligned} \overline{P}_{se}^{MIMO} = {} & 2q(M_I)\int_{\mathbf{\Gamma}} Q(A_I\sqrt{\gamma})\, f_{\mathbf{\Gamma}}(\Gamma)d\Gamma \\ & + 2q(M_Q)\int_{\mathbf{\Gamma}} Q(A_Q\sqrt{\gamma})\, f_{\mathbf{\Gamma}}(\Gamma)d\Gamma \\ & - 4q(M_I)q(M_Q)\int_{\mathbf{\Gamma}} Q(A_I\sqrt{\gamma})Q(A_Q\sqrt{\gamma})\, f_{\mathbf{\Gamma}}(\Gamma)d\Gamma. \end{aligned} \tag{18}$$

Assuming that MIMO sub-channels' turbulence processes are uncorrelated, independent and identically distributed (i.i.d.), the joint p.d.f $f_{\mathbf{\Gamma}}(\Gamma)$ can be reduced to a product of the first-order p.d.f of each element Γ_{mn} [33]. From Eqs. (7), (8) and (12), the p.d.f of the r.v. Γ_{mn} in case of weak/moderate and strong turbulence channels can be, respectively, given as

$$f_{\Gamma_{mn}}(\gamma_{mn}) = \frac{1}{2\gamma_{mn}\sigma_s\sqrt{2\pi}} \exp\left(-\frac{\left(\ln(\frac{\gamma_{mn}}{\overline{\gamma}_{mn}}) + \sigma_s^2\right)^2}{8\sigma_s^2}\right), \tag{19}$$

and,

$$f_{\Gamma_{mn}}(\gamma_{mn}) = \frac{(\alpha\beta)^{\frac{\alpha+\beta}{2}}}{\Gamma(\alpha)\Gamma(\beta)} \frac{\gamma_{mn}^{\frac{\alpha+\beta}{4}-1}}{\overline{\gamma}_{mn}^{\frac{(\alpha+\beta)}{4}}} K_{\alpha-\beta}\left(2\sqrt{\alpha\beta\sqrt{\frac{\gamma_{mn}}{\overline{\gamma}_{mn}}}}\right). \tag{20}$$

3.2 Average Channel Capacity

In this section, we analytically derive the average channel capacity (ACC) for the $M\times N$ MIMO/FSO link in the presence of atmospheric turbulences. This is a crucial metric for evaluating the optical link performance. The ACC can also be expressed in terms of average spectral efficiency (ASE) in bits/s/Hz if the frequency response of the channel is known. We assume that the optical channel is memoryless, stationary, ergodic with i.i.d. turbulence statistics and perfect channel state information (CSI) is available at both the transmitting lasers and the aperture receivers, the system ASE can be defined as

$$\frac{\overline{C}}{B} = \int_{\mathbf{\Gamma}} \log_2(1+\gamma) f_{\mathbf{\Gamma}}(\Gamma) d\Gamma, \quad \text{(bit/s)} \tag{21}$$

where B is the channel's bandwidth and γ is the total channel SNR as given in Eq. (6) and $\mathbf{\Gamma} = \{\Gamma_{nm}, n = 1, ..., N, m = 1, ..., M\}$ is the matrix of the MIMO atmospheric turbulence channels. Similarly, the joint p.d.f $f_{\mathbf{\Gamma}}(\Gamma)$ can be reduced to a product of the first-order p.d.f of each element Γ_{mn}. The p.d.f of the r.v. Γ_{mn} in case of log-normal and gamma-gamma channels are given in Eqs. (19) and (20), respectively. As a result, the system ASE expressed in Eq. (21) can be calculated through multi-dimensional numerical integration.

3.2.1 Capacity of Log-normal MIMO/FSO Channels

Using (19) and (21), the ASE of a log-normal MIMO/FSO channel can be expressed as

$$\begin{aligned} \frac{\overline{C}}{B} = {} & \frac{1}{2\sigma_s\sqrt{2\pi}\ln(2)} \int_{\mathbf{\Gamma}} \frac{\ln(1+\gamma_{mn})}{\gamma_{mn}} \\ & \times \exp\left(-\frac{\left(\ln(\frac{\gamma_{mn}}{\overline{\gamma}_{mn}}) + \sigma_s^2\right)^2}{8\sigma_s^2}\right) d\gamma_{mn}. \end{aligned} \tag{22}$$

Using the equality $\ln(1+x) = \sum_{k=1}^{+\infty}(-1)^{k+1}x^k/k$, $(0 \le x \le 1)$, and the scaled complementary error function erfcx(x)=

$$\frac{\overline{C}}{B} = C_0\left\{\sum_{k=1}^{\infty}\frac{(-1)^{k+1}}{k}\left[\mathrm{erfcx}\left(\sqrt{2}\sigma_s k+\frac{\Gamma_{mn}}{2\sqrt{2}\sigma_s}\right)+\mathrm{erfcx}\left(\sqrt{2}\sigma_s k-\frac{\Gamma_{mn}}{2\sqrt{2}\sigma_s}\right)\right]+\frac{4\sigma_s}{\sqrt{2\pi}}+\Gamma_{mn}\exp\left(\frac{\Gamma_{mn}^2}{8\sigma_s^2}\right)\mathrm{erfcx}\left(-\frac{\Gamma_{mn}}{2\sqrt{2}\sigma_s}\right)\right\}, \tag{23}$$

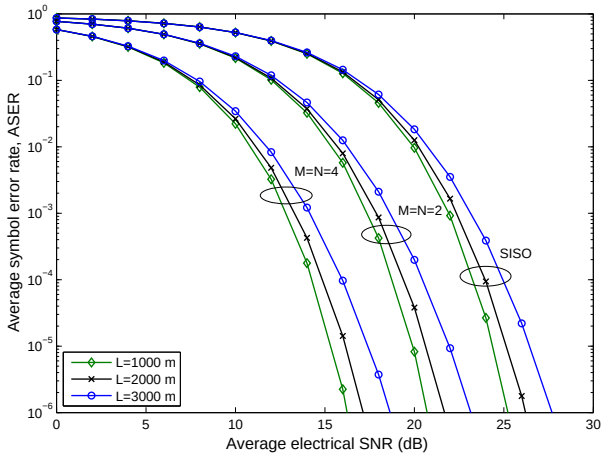

Fig. 3 ASER versus average SNR, $\overline{\gamma}$, of SISO/FSO system, 2x2 and 4x4 MIMO/FSO systems for various values of L using 8×4 QAM, $C_n^2 = 10^{-15}$ m$^{-2/3}$

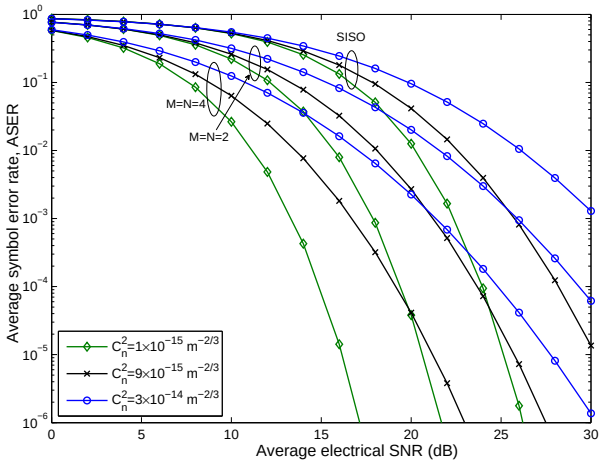

Fig. 4 ASER versus the average SNR, $\overline{\gamma}$, of SISO/FSO system, 2x2 and 4x4 MIMO/FSO systems for various values of C_n using 8×4 QAM, $L =$ 2000 m

$e^{x^2}\mathrm{erfc}(x)$, the integral (22) can be transformed to the summation in Eq. (23). In Eq. (23), $\Gamma_{mn} = \ln(\overline{\gamma}_{mn}) - \sigma_s^2$ with $\overline{\gamma}_{mn}$ is the instantaneous received SNR output of EGC detector, and $C_0 = \exp(-\Gamma^2/8\sigma_s^2)/2\ln 2$.

3.2.2 Capacity of Gamma-Gamma MIMO/FSO Channels

Substituting (20) into (21), the average capacity of a gamma-gamma MIMO/FSO channel can be given by

$$\frac{\overline{C}}{B} = \frac{\left(\frac{\alpha\beta}{\sqrt{\overline{\gamma}_{mn}}}\right)^{\frac{\alpha+\beta}{2}}}{\Gamma(\alpha)\Gamma(\beta\ln(2)}\int_{\Gamma}\ln(1+\gamma_{mn}) \times\gamma_{mn}^{\frac{\alpha+\beta}{4}-1}K_{\alpha-\beta}\left(2\sqrt{\alpha\beta}\sqrt{\frac{\gamma_{mn}}{\overline{\gamma}_{mn}}}\right)d\gamma_{mn}. \tag{24}$$

Using the Meijer G-function, $\mathrm{G}_{mn}^{pq}[\cdot]$, to express the logarithmic term of $\ln(1+x) = \mathrm{G}_{2,2}^{1,2}\left[x\middle|_{1,0}^{1,1}\right]$ ([34], eq. (11)), and $K_\vartheta(x) = \frac{1}{2}\mathrm{G}_{0,2}^{2,0}\left[\frac{x^2}{4}\middle|_{\frac{\vartheta}{2},-\frac{\vartheta}{2}}^{-,\ -}\right]$ ([34], eq. (14)), the ASE can be expressed by

$$\frac{\overline{C}}{B} = \frac{\left(\frac{\alpha\beta}{\sqrt{\overline{\gamma}_{mn}}}\right)^{c/2}}{4\pi\Gamma(\alpha)\Gamma(\beta)\ln(2)}\mathrm{G}_{2,6}^{6,1}\left[\frac{(\alpha\beta)^2}{16\overline{\gamma}_{mn}}\middle|_{\frac{d}{4},\frac{d+2}{4},-\frac{d}{4},-\frac{c}{4},-\frac{c}{4}}^{-\frac{c}{4},-\frac{c}{4}+1}\right], \tag{25}$$

where $c = \alpha + \beta$ and $d = \alpha - \beta$.

4. Numerical Results

In the following analysis, we evaluate the ASER for different values of C_n^2: 1×10^{-15} m$^{-2/3}$, 9×10^{-15} m$^{-2/3}$, and 3×10^{-14} m$^{-2/3}$ for weak, moderate, and strong turbulence conditions, respectively. As mentioned earlier, the log-normal distribution model is used for the case of weak turbulence; whereas the gamma-gamma distribution model is used for cases of moderate to strong turbulence. In addition, we consider the receiver aperture with diameter $D = 0.08$ m, and the operational wavelength $\lambda = 1.55$ μm, while the distances L of 1000 m, 2000 m, and 3000 m are chosen for the free-space links. It is noted that the influence of the atmospheric turbulence conditions has slight effect to the system performance when the link distance is shorter than 1000 m.

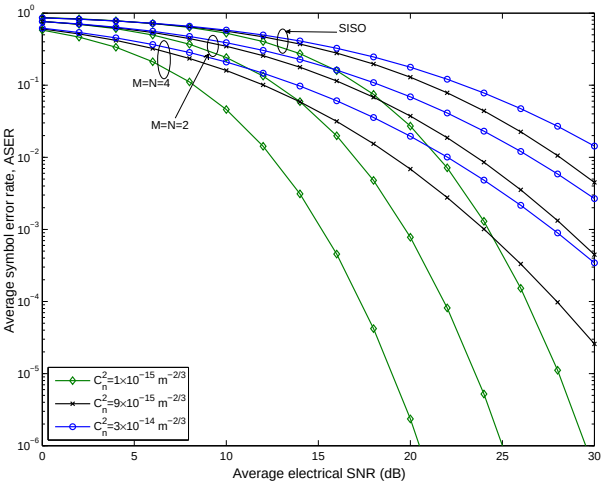

Fig. 5 ASER versus the average SNR, $\overline{\gamma}$, of SISO/FSO system, 2x2 and 4x4 MIMO/FSO systems for various values of C_n using 8×4 QAM, $L =$ 4000 m

Fig. 3 illustrates the ASER as a function of the average electrical SNR, $\overline{\gamma} = (\frac{1}{MN}a\Re P_s\kappa)^2/N_0$, for different values

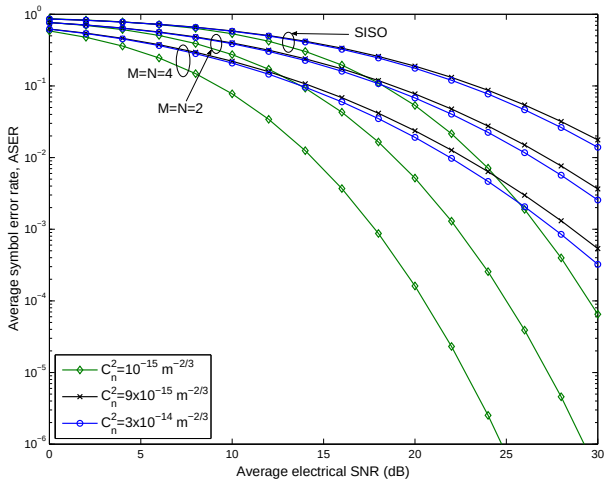

Fig. 6 ASER versus the average SNR, $\overline{\gamma}$, of SISO/FSO system, 2x2 and 4x4 MIMO/FSO systems for various values of C_n using 8×4 QAM, L = 6000 m

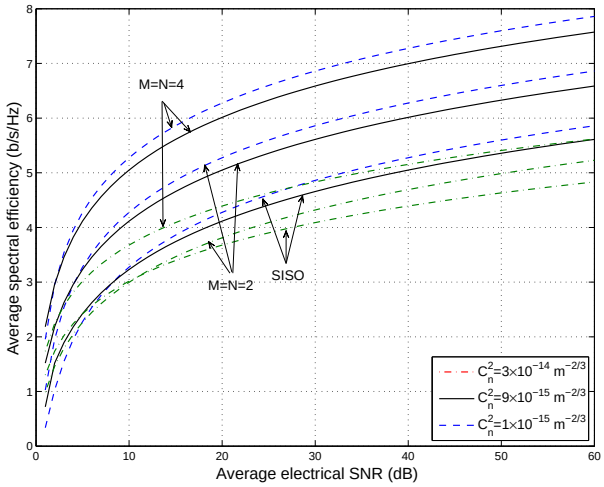

Fig. 8 ASE, $\overline{C}/B$, versus the average electrical SNR, $\overline{\gamma}$, of different MIMO/FSO channels for weak to strong turbulence strength, C_n^2, the link length L=3000 m

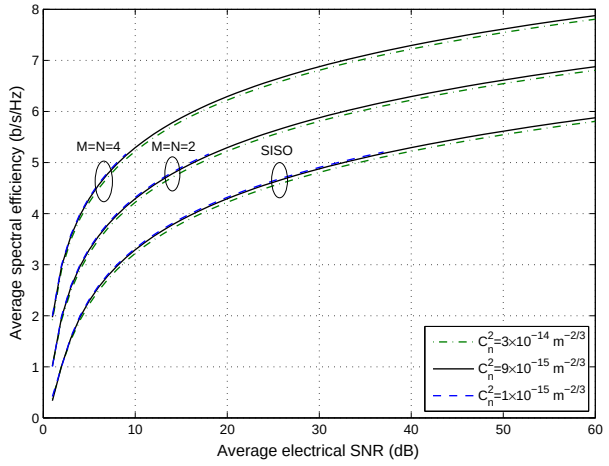

Fig. 7 ASE, $\overline{C}/B$, versus the average electrical SNR, $\overline{\gamma}$, of different MIMO/FSO channels for weak to strong turbulence strength, C_n^2, the link length L = 1000 m

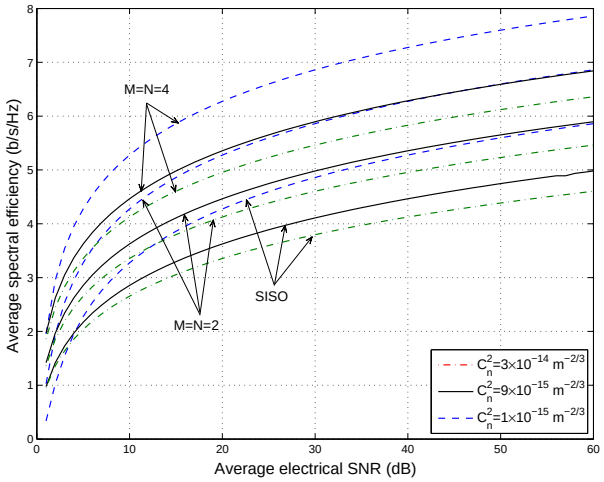

Fig. 9 ASE, $\overline{C}/B$, versus the average electrical SNR, $\overline{\gamma}$, of different MIMO/FSO channels for weak to strong turbulence strength, C_n^2, the link length L=6000 m

of link distance L. We consider different MIMO configurations of 2×2 and 4×4 for FSO systems using SC-QAM over weak turbulence with $C_n^2 = 1 \times 10^{-15}$ m$^{-2/3}$. The performance of SISO/FSO SISO system (i.e. $(M = N = 1)$) is also included in Fig. 3 as a benchmark. As it is clearly shown, the performance is improved significantly with the increase of number of lasers and receivers, which, as a result, could increases the transmission link distance. More specifically, when the link distance L increases from 1000 m to 2000 m and 3000 m, a significant error performance degradation is observed for the same SNR. However, as expected, ASER decreases as number of lasers M and receiver N increase from $M = N = 2$ to $M = N = 4$. It is seen in Fig. 3 that, in case of L = 2000 m, when the MIMO configuration changes from SISO to 2×2 MIMO or 2×2 MIMO to 4×4 MIMO, it results in an average gain of approximately 5 dB at the ASER of 10^{-6}.

In Figs. 4–6, the impacts of the turbulence strength C_n^2 on the error performance of various system configurations with different link distances $L = 2000, 4000, 6000$ m are analyzed. As can be observed in Fig. 4, when L = 2000 m the systems' performance depends strongly on the value of C_n^2. For example, to get the ASER = 10^{-6} the 4×4 MIMO/FSO system increases $\overline{\gamma}$ = 6 dB and 7 dB from weak to moderate and from moderate to strong cases, respectively. We also can obtain this ASER value by adding about 5 dB and 10 dB for 2×2 MIMO/FSO and SISO systems, respectively. In addition, by comparing these three figures, it is seen that the ASER also strongly depends on the link distance. In particular, for the 4×4 MIMO/FSO system with the weak turbulence strength $C_n^2 = 1 \times 10^{-15}$, the average electrical SNRs required to achieve the ASER of 10^{-6} for $L = 2000, 4000$ and 6000 are 17, 20.5 and 24.5 dB, respectively.

Next, using the closed-form expressions of (23) and (25), we evaluate the ASE of MIMO/FSO channels as a function of the average electrical SNR at the receiver, $\overline{\gamma}$. We use (23) for the cases of weak turbulence with log-normal distribution model, while (25) is used for moderate to strong cases with the gamma-gamma distribution. We use the system parameters and three different values of turbulence strength and link distance, C_n^2, L, as discussed above. Here again, SISO/FSO channel is also included in the numerical results as a benchmark.

Figures 7–9 illustrate the ASE of different MIMO/FSO channels (i.e., 2×2 and 4×4 MIMO/FSO channels) with respect to $\overline{\gamma}$, for three values of the turbulence strength C_n^2 (i.e., $C_n^2 = 1 \times 10^{-15}$ m$^{-2/3}$, $C_n^2 = 9 \times 10^{-15}$ m$^{-2/3}$, and $C_n^2 = 3 \times 10^{-14}$ m$^{-2/3}$, for weak, moderate and strong turbulence conditions, respectively), and with three different link distances ($L = 1000, 3000$ m, and 6000 m). It can be also seen that the ASE strongly depends on the atmospheric turbulence strength, and as the link distance gets longer, the influence of atmospheric turbulence becomes stronger. Obviously, the ASE under the weak turbulence conditions is higher than in the cases of moderate and strong turbulence, especially with longer link distance L. The reason of this is that as optical link distance gets longer, the signal propagates in the atmospheric with longer distances, the influence of the turbulence therefore becomes stronger. On the other hand, as expected, the ASE could be improved by approximately 1 (b/s/Hz) when the system is upgraded from SISO/FSO to 2×2 MIMO/FSO or from 2×2 MIMO/FSO to 4×4 MIMO/FSO.

5. Conclusions

We have presented the performance analysis on the average channel capacity and ASER of MIMO/FSO systems using SC-QAM signaling over atmospheric turbulence channels. The log-normal and gamma-gamma distribution models were used to describe the fluctuation of the optical propagating over atmospheric turbulence channels. We analytically derived the system ASER and ASE considering different link conditions and MIMO configurations. The numerical results showed that, with the similar link distance and turbulence strength, when the FSO system is upgraded from SISO to 2×2 MIMO or 2×2 MIMO to 4×4 MIMO, an average gain of approximately 5 dB at the ASER of 10^{-6} could be obtained. As well, regardless the link distance and turbulence condition, the ASE of the FSO link could be improved by approximately 1 (b/s/Hz) when the system is upgraded from from SISO/FSO to 2×2 MIMO/FSO or from 2×2 MIMO/FSO to 4×4 MIMO/FSO.

References

[1] H. Willebrand and B. S. Ghuman, *Free Space Optics: Enabling Optical Connectivity in Today's Networks*. Indianapolis, IN: Sams Publishing, 2002.

[2] D. Kedar and S. Arnon, "Urban optical wireless communication networks: The main challenges and possible solutions," *IEEE Commun. Mag.*, vol.42, no.5, pp.2–7, May 2004.

[3] H. Haas, S. Imre, D. O'Brien, M. Rupp, and L. Gyongyosi, "Wireless Myths, Realities, and Futures: From 3G/4G to Optical and Quantum Wireless," *Proceedings of the IEEE*, vol.100 , no.13, pp.1853–1888, May 2012.

[4] V. Kvicera, M. S. Awan, E. Leitgeb, S. Muhammad, and G. Kandus, "Weather effects on hybrid FSO/RF communication link," *IEEE J.Sel. Areas in Communications*, vol.7, no.9, pp.1687–1697, Dec. 2009.

[5] X. Zhu and J. M. Kahn, "Free-space optical communication through atmospheric turbulence channels," *IEEE Trans. Commun.*, vol.50, no.8, pp.1293–1300, Aug. 2002.

[6] L. Andrews, R. L. Philips, and C. Y. Hopen, *Laser Beam Scintillation With Applications*. SPIE Press, 2001.

[7] X. Zhu and J. M. Kahn, "Performance bounds for coded free-space optical communications through atmospheric turbulence channels," *IEEE Trans. Commun.*, vol.51, no.8, pp.1233–1239, Aug. 2003.

[8] M. Uysal, J. Li, and M. Yu, "Error rate performance analysis of coded free-space optical links over gamma-gamma atmospheric turbulence channels," *IEEE Trans. Wirel. Commun.*, vol.5, no.6, pp.1229–1233, Jun. 2006.

[9] M. M. Ibrahim and A. M. Ibrahim, "Performance analysis of optical receivers with space diversity reception," *Proc. IEE-Commun.*, vol.143, no.6, pp.369–372, Dec. 1996.

[10] E. Lee and V. Chan, "Part 1: Optical communication over the clear turbulence atmospheric channel using diversity," *IEEE Trans. Commun.*, vol.22, no.9, pp.1896–1960, Nov. 2004.

[11] E. J. Shin and V. W. S. Chan, "Optical communication over the turbulent atmospheric channel using spatial diversity," *IEEE GLOBECOM*, pp.2055–2060, Nov. 2002,

[12] S. G. Wilson, M. Brandt-Pearce, Q. Cao, and J. H. Leveque, "Free-space optical MIMO transmission with Q-ary PPM," *IEEE Trans. Commun.*, vol.53, no.8, pp.1402–1412, Aug. 2005.

[13] S. G. Wilson, M. Brandt-Pearce, Q. Cao, and J. H. Leveque, "Optical repetition MIMO transmission with multiple PPM," *IEEE J. Sel. Areas Commun.*, vol.23, no., pp.1901–1910, Sept. 2005.

[14] S. M. Navidpour, M. Uysal, and M. Kavehrad, "BER performance of free-space optical transmission with diversity," *IEEE Trans. on Wireless Commun.*, vol.6, no.8, pp.1402–1412, Aug. 2007.

[15] T. A. Tsiftsis, H. G. Sandalidis, G. K. Karagiannidis, and M. Uysal, "FSO links with spatial diversity over strong atmospheric turbulence channels," in Proc. *ICC '08*, pp.5379–5384, May 2008

[16] W. Huang, J. Takayanagi, T. Sakanaka, and M. Nakagawa, "Atmospheric optical communication system using subcarrier PSK modulation," *IEICE Trans. Commun.*, vol.E76-B, pp.1169–1177, Sep. 1993.

[17] J. Li, J. Q. Liu, and D. P. Taylor, "Optical communication using subcarrier PSK intensity modulation through atmospheric turbulence channels," *IEEE Trans. Commun.*, vol.55, pp.1598–1606, Aug. 2007.

[18] W. O. Popoola, Z. Ghassemlooy, J. I. Allen, E. Leitgeb, and S. Gao, "Free-space optical communication employing subcarrier modulation and spatial diversity in atmospheric turbulence channel," *IET Optelectron.*, vol.2, pp.16–23, Feb. 2008.

[19] W. O. Popoola and Z. Ghassemlooy, "BPSK subcarrier intensity modulated free-space optical communications in atmospheric turbulence," *J. Lightwave Technol.*, vol.27, pp.967–973, Apr. 2009.

[20] A. Pham, T. Thang, S. Guo, and Z. Cheng, "Performance bounds for turbo-coded sc-psk/fso communications overstrong turbulence channels," in *IEEE International Conference on Advanced Technologies for Communications (ATC'11)*, Aug. 2011, pp.161–164.

[21] J. Park, E. Lee, and G. Yoon, "Average bit-error rate of the Alamouti scheme in Gamma-Gamma fading channels," *IEEE Phton. Technol. Lett.*, vol.23, pp.269–271, Feb. 2011.

[22] X. Song, M. Niu, and J. Cheng, "Error rate of subcarrier intensity modulations for wireless optical communications," *IEEE Commun. Lett.*, vol.16, pp.540–543, Apr. 2012.

[23] N. Cvijetic and T. Wang, "WiMAX over free-space optics-evaluating OFDM multi-subcarrier modulation in optical wireless channels," in *IEEE Sarnoff Symp.*, Mar. 2006, pp.1–4.
[24] A. Bekkali, C. B. Naila, K. Kazaura, K. Wakamori, and M. Matsumoto, "Transmission analysis of OFDM-based wireless services over turbulent radio-on-fso links modeled by gamma-gamma distribution," *IEEE Photonics J.*, vol.3, no.3, pp.510–520, Jun. 2010.
[25] Md. Z. Hassan, X. Song, and J. Cheng, "Subcarrier intensity modulated wireless optical communications with rectangular QAM," *J. Opt. Commun. Netw*, vol.4, no.6, pp.522–532, Jun. 2012.
[26] E. Bayaki, R. Schober, and R. K. Mallik, "Performance of MIMO free-space optical systems in gamma-gamma fading," *IEEE Trans. Commun.*, vol.57, no.11, pp.3415–3424, Nov. 2009.
[27] K. P. Peppas and C. K. Datsikas, "Average symbol error probability of general-order rectangular quadrature amplitude modulation of optical wireless communication systems over atmospheric turbulence channels," *J. Opt. Commun. Netw.*, vol.1, no.2, pp.102–110, Feb. 2010.
[28] M. Z. Hassan, X. Song, and J. Cheng, "Subcarrier intensity modulated wireless optical communications with rectangular QAM," *J. Opt. Commun. Netw.*, vol.4, no.6, pp.522–532, Jun. 2012.
[29] Vu, B.T.; Truong, C.T.; Pham, A.T.; Dang, N.T., "Performance of rectangular QAM/FSO systems using APD receiver over atmospheric turbulence channels," *TENCON 2012 - 2012 IEEE Region 10 Conference,* pp.1–5, 19-22 Nov. 2012.
[30] Vu, B.T.; Dang, N.T.; Truong, C.T.; Pham, A.T., "Bit-Error Rate Analysis of Rectangular QAM/FSO Systems using APD Receiver Over Atmospheric Turbulence Channels," *IEEE/OSA Journal of Optical Communications and Networking* 2013 (to appear).
[31] A. K. Majumdar, "Free-space laser communication performance in the atmospheric channel," *J. Opt. Fiber Commun. Rep.*, vol.2, no.4, pp.345–396, 2005.
[32] A. Maaref and S. Aissa, "Exact error probability analysis of rectangular QAM for single- and multichannel reception in Nakagami-m fading channels," *IEEE Trans. Commun.*, vol.57, no.1, pp.214–221, Jan. 2009.
[33] Cvijetic, N., Wilson, S.G.; Brandt-Pearce, M., "Performance Bounds for Free-Space Optical MIMO Systems with APD Receivers in Atmospheric Turbulence." *Selected Areas in Communications, IEEE Journal on*, vol.26, no.3, pp.3–12, Apr. 2008.
[34] V. S. Adamchik, and O. I. Marichev, "The algorithm for calculating integrals of hypergeometric type functions and its realization in reduce system," in *Int. Conf. on Symbolic and Algebraic Computation*, Tokyo, Japan, 1990, pp.212–224.

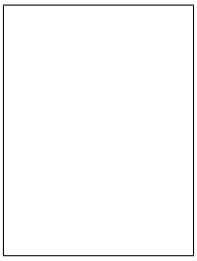

Ha D. Trung was born in Thanh Hoa, Vietnam in 1980. He received the B.Eng. degree in Electronics and Telecommunications from Hanoi University of Technology, Vietnam, and the MS and PhD degrees in Communications Engineering from Chulalongkorn University, Bangkok, Thailand in 2005 and 2009, respectively. Since September 2009, he has been an assistant professor at the School of Electronics and Telecommunications, Hanoi University of Science and Technology. In 2012, Dr. Trung spent 3 months as a visiting researcher at the University of Aizu, Japan. His present research interests are in the area of Free-Space Optical and MIMO communications, GNSS technology and its applications. Dr. Trung received Japanese International Cooperation Agency (JICA) scholarship for his MS and PhD studies.

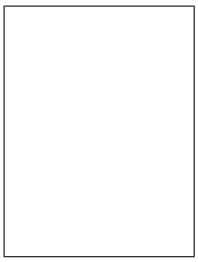

Anh T. Pham received the B.E. and M.E. degrees, both in Electronics Engineering from the Hanoi University of Technology, Vietnam in 1997 and 2000, respectively, and the Ph.D. degree in Information and Mathematical Sciences from Saitama University, Japan in 2005. From 1998 to 2002, he was with the NTT Corp. in Vietnam. Since April 2005, he has been on the faculty at the University of Aizu, where he is currently a senior associate professor at the Computer Communications Laboratory, the School of Computer Science and Engineering. His present research interests are in the area of computer networking, optical communications, and spread spectrum technique. Dr. Pham received Japanese government scholarship (MonbuKagaku-sho) for Ph.D. study. He also received Vietnamese government scholarship for undergraduate study. Dr. Pham is senior member of IEEE. He is also member of IEICE and OSA.